Catalysis and Binding in L-Ribulose-5-Phosphate 4-Epimerase: A Comparison with L-Fuculose-1-Phosphate Aldolase[†,‡]

Jomy Samuel,[§] Yu Luo,[||] Paul M. Morgan,[§] Natalie C. J. Strynadka,[||] and Martin E. Tanner*[,§]

Department of Chemistry, University of British Columbia, Vancouver, British Columbia, Canada V6T 1Z1, and Department of Biochemistry and Molecular Biology, University of British Columbia, Vancouver, British Columbia, Canada V6T 1Z3

Received June 18, 2001; Revised Manuscript Received September 24, 2001

ABSTRACT: L-Ribulose-5-phosphate (L-Ru5P) 4-epimerase and L-fuculose-1-phosphate (L-Fuc1P) aldolase are evolutionarily related enzymes that display 26% sequence identity and a very high degree of structural similarity. They both employ a divalent cation in the formation and stabilization of an enolate during catalysis, and both are able to deprotonate the C-4 hydroxyl group of a phosphoketose substrate. Despite these many similarities, subtle distinctions must be present which allow the enzymes to catalyze two seemingly different reactions and to accommodate substrates differing greatly in the position of the phosphate (C-5 vs C-1). Asp76 of the epimerase corresponds to the key catalytic acid/base residue Glu73 of the aldolase. The D76N mutant of the epimerase retained considerable activity, indicating it is not a key catalytic residue in this enzyme. In addition, the D76E mutant did not show enhanced levels of background aldolase activity. Mutations of residues in the putative phosphate-binding pocket of the epimerase (N28A and K42M) showed dramatically higher values of K_M for L-Ru5P. This indicates that both enzymes utilize the same phosphate recognition pocket, and since the phosphates are positioned at opposite ends of the respective substrates, the two enzymes must bind their substrates in a reversed or "flipped" orientation. The epimerase mutant D120N displays a 3000-fold decrease in the value of k_{cat}, suggesting that Asp120′ provides a key catalytic acid/base residue in this enzyme. Analysis of the D120N mutant by X-ray crystallography shows that its structure is indistinguishable from that of the wild-type enzyme and that the decrease in activity was not simply due to a structural perturbation of the active site. Previous work [Lee, L. V., Poyner, R. R., Vu, M. V., and Cleland, W. W. (2000) *Biochemistry 39*, 4821−4830] has indicated that Tyr229′ likely provides the other catalytic acid/base residue. Both of these residues are supplied by an adjacent subunit. Modeling of L-Ru5P into the active site of the epimerase structure suggests that Tyr229′ is responsible for deprotonating L-Ru5P and Asp120′ is responsible for deprotonating its epimer, D-Xu5P.

L-Ribulose-5-phosphate 4-epimerase (AraD, EC 5.1.3.4) catalyzes the interconversion of L-ribulose 5-phosphate (L-Ru5P)[1] and D-xylulose 5-phosphate (D-Xu5P) (Figure 1A). The enzyme employs a mechanism involving an initial retroaldol cleavage between C-3 and C-4 of the substrate that generates glycolaldehyde phosphate and the metal-bound enolate of dihydroxyacetone as intermediates (*1*−*3*). A subsequent aldol addition of the same face of the enolate to the opposite face of the aldehyde generates the epimeric product. This mechanistic proposal is consistent with the notion that the epimerase is evolutionarily related to the class II aldolase, L-fuculose-1-phosphate (L-Fuc1P) aldolase (Figure 1B) (*4*−*6*). The two enzymes appear to belong to a superfamily of epimerases/racemases (including L-rhamnulose-1-phosphate aldolase) that have retained the ability to generate enolate ions via aldol chemistry. They are known to share limited sequence identity (26%), and they both employ three conserved histidine residues as ligands for an active site divalent metal ion. In the previous paper, we have presented a structural analysis of the crystallized *E. coli* L-Ru5P 4-epimerase that pointed out the remarkable structural similarity it shares with the *E. coli* L-Fuc1P aldolase (*7*).

Despite the fact that the enzymes share a common fold and catalyze mechanistically similar reactions, the structures of the substrates demand that there be significant differences in the residues involved in binding and/or catalysis. In both

[†] This research was supported in part by the Natural Sciences and Engineering Research Council of Canada (NSERC) (operating grant to M.E.T.) and the Canadian Institute of Health Research and Howard Hughes Medical Institute (to N.C.J.S.).

[‡] X-ray coordinates have been deposited in the Protein DataBank (PDB accession code 1KOW).

* To whom correspondence should be addressed. Phone: (604) 822-9453, fax: (604) 822-2847, e-mail: mtanner@chem.ubc.ca.

[§] Department of Chemistry, University of British Columbia.

[||] Department of Biochemistry and Molecular Biology, University of British Columbia.

[1] Abbreviations: L-Ru5P, L-ribulose 5-phosphate; D-Xu5P, D-xylulose 5-phosphate; L-Fuc1P, L-fuculose 1-phosphate; PCR, polymerase chain reaction; MWCO, molecular weight cutoff; SDS−PAGE, sodium dodecyl sulfate−polyacrylamide gel electrophoresis; ESI-MS, electrospray ionization mass spectrometry; EDTA, ethylenediaminetetraacetic acid; HEPES, *N*-(2-hydroxyethyl)piperazine-*N*′-2-ethanesulfonic acid; LB, Luria broth; DTT, dithiothreitol; PMSF, phenylmethylsulfonyl fluoride; ATP, adenosine 5′-triphosphate; NMR, nuclear magnetic resonance; TPP, thiamin pyrophosphate; α-GDH, α-glycerophosphate dehydrogenase; DHA, dihydroxyacetone; Tris, tris(hydroxymethyl)-aminomethane; NAD^+/NADH, nicotinamide adenine dinucleotide/dihydronicotinamide adenine dinucleotide; CD, circular dichroism; WT, wild-type.

10.1021/bi011252v CCC: $20.00
Published on Web 11/09/2001

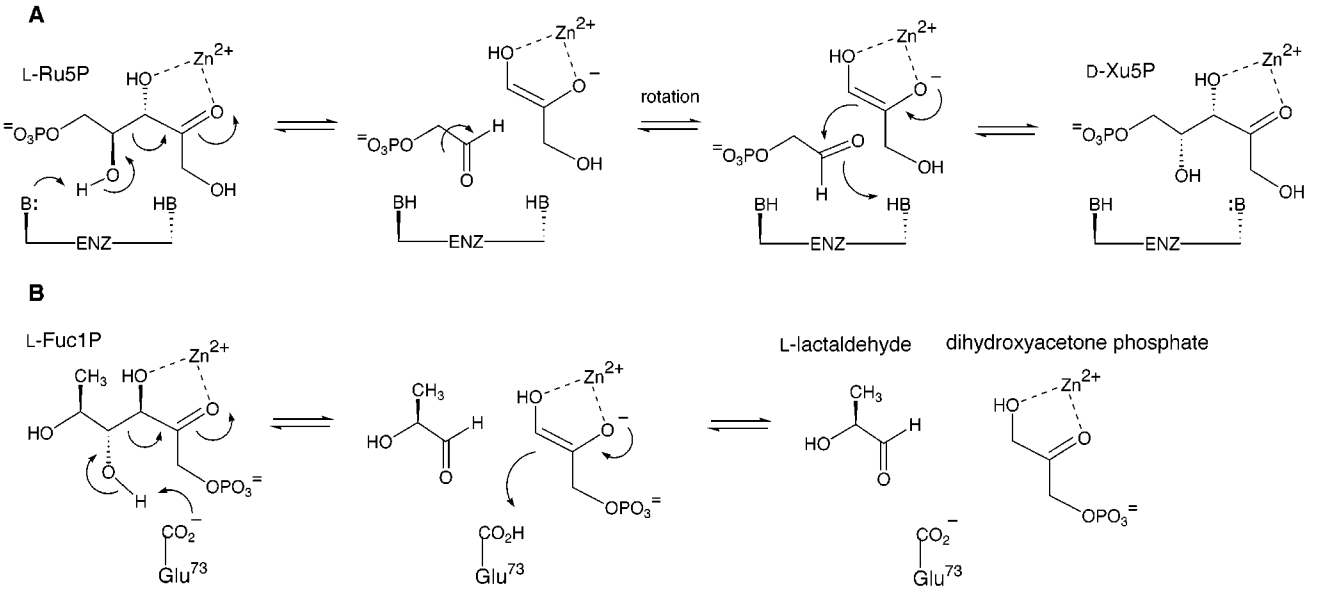

FIGURE 1: (A) Mechanism of the reaction catalyzed by L-ribulose-5-phosphate 4-epimerase. (B) Mechanism of the reaction catalyzed by L-fuculose-1-phosphate aldolase.

reactions, the metal serves as an electrophilic catalyst and must be coordinated to the ketone oxygen at C-2 to promote enolate formation (Figure 1). In addition, both enzymes must position catalytic acid/base residues appropriately to deprotonate a hydroxyl group at C-4 of the respective substrates (two such residues are presumably required for the epimerase, one for each epimer). However, the phosphate of L-Fuc1P is located on the hydroxyl at C-1 whereas that of L-Ru5P is at C-5. Since the phosphate is likely a key determinant in the recognition and binding of these substrates, it is reasonable to assume that the enzymes would evolve a distinct phosphate-binding pocket. This is certainly the case with the aldolase, and it is important to note that the residues in the phosphate-binding pocket of the aldolase are strictly conserved in the epimerase (*5*, *7*). If these residues play a similar role in the epimerase, the substrate would have to bind in a reversed orientation, and the acid/base residue(s) corresponding to those in the aldolase would be miss-positioned to participate in catalysis. In this paper we use site-directed mutagenesis to probe whether the phosphate-binding pocket or the residues serving as acid/base catalysts are preserved between the two enzymes. We also describe further studies on the background aldolase activity of the epimerase, an observation that provided the initial evidence for the retro-aldol/aldol mechanism with this enzyme.

EXPERIMENTAL PROCEDURES

Materials and General Procedures. The pTrc99A expression vector used for cloning ribulokinase was from Pharmacia. Restriction enzymes *Eco*RI, *Pst*I, and *Bam*HI were from Promega while *Nco*I was from New England BioLabs. T4 DNA ligase and dNTP mix were from Gibco BRL. The protease inhibitors pepstatin and aprotinin were from Boehringer Mannheim. PWO polymerase was from Roche Diagnostics. Ampicillin was from Fisher Scientific. All other coupling enzymes and chemicals were from Sigma or Aldrich Chemical Co. The Wizard Miniprep DNA purification kit from Promega was used for all plasmid purifications.

Preparation of Mutant Plasmids. Plasmid pRE1, an expression vector that encodes for the *araD* gene, was used as a template for all mutagenesis experiments. The D76E mutant was prepared by recombinant circle PCR (RCPCR) (*8*), and the primers used were JS01 (5′-G CCC TCC TCC GAG ACC CCA ACT CAC C-3′) and JS02 (antiparallel) (5′-G GTG AGT TGG GGT CTC GGA GGA GGG C-3′) (sites of mutation are underlined). The double-stranded template plasmid was cut, in two separate reactions, using the restriction endonucleases *Eco*RI and *Pst*I to give two linearized plasmids. Primers JS01 and MT09 (antiparallel) (5′-GCA GAG CGA GGT ATG TAG GCG GTG-3′) were used to amplify the plasmid cut with *Eco*RI. Primers MT08 (5′-CGA CGA GCG TGA CAC CAC GAT GCC-3′) and JS02 (antiparallel) were used to amplify the plasmid cut with *Pst*I. PCR was carried out using PWO polymerase under the following conditions: 1 cycle of 2 min at 96 °C; 10 cycles of 1 min at 96 °C, 45 s at 60 °C, and 2 min at 72 °C; 10 cycles of 1 min at 96 °C, 45 s at 55 °C, and 2 min at 72 °C; 10 cycles of 1 min at 96 °C, 45 s at 50 °C, and 2 min at 72 °C, followed by 7 min at 72 °C. Equal volume aliquots of the two crude PCR reactions were then combined, denatured (3 min at 94 °C), and annealed (2 h at 50 °C) prior to transformation into $CaCl_2$-competent *E. coli* DH5α (Gibco/BRL). Individual colonies that grew on LB−agar plates supplemented with 100 μg/mL ampicillin were used to inoculate a 5 mL overnight culture of LB containing 100 μg/mL ampicillin. Plasmid DNA was isolated to give pJSTB1 encoding for the D76E mutation. All other mutants were prepared according to the protocol of the QuickChange Site-Directed Mutagenesis Kit from Stratagene. Oligonucleotide pairs that were used to introduce mutation in the forward and reverse directions are listed below, with the mutated nucleotides underlined. Primers used for the T116Y mutant are JS07 (5′-CCA GCA ACC GGC TAC ACC CAC GCC GAC T-3′) and JS08 (antiparallel) (5′-A GTC GGC GTG GGT GTA GCC GGT TGC TGG-3′). Primers used for T116E mutant are JS09 (5′-CCA GCA ACC GGC GAG ACC CAC GCC GAC T-3′) and JS10 (antiparallel) (5′-A GTC GGC GTG GGT CTC GCC GGT TGC TGG-3′). Primers used for the E142Q mutant are JS11 (5′-C AAC

GGC GAA TAT CAG TGG GAA ACC G-3′) and JS12 (antiparallel) (5′-CC GGT TTC CCA CTG ATA TTC GCC GTT G-3′). Primers used for the H218N mutant are JS13 (5′-CG CTG CTG GAT AAA AAC TAT CTG CGT AAG C-3′) and JS14 (antiparallel) (5′-GCC ATG CTT ACG CAG ATA GTT TTT ATC CAG CAG-3′). Primers used for the D120N mutant are JS15 (5′-GGC ACC ACC CAC GCC AAC TAT TTC TAC GGC-3′) and JS16 (antiparallel) (5′-GGT GCC GTA GAA ATA GTT GGC GTG GG-3′). Primers used for the N28A mutant are JS17 (5′-CTC ACA TGG GGC GCC GTC AGC GCC G-3′) and JS18 (antiparallel) (5′-C GCT GAC GGC GCC CCA TGT GAG CGT-3′). Primers used for the K42M mutant are JS19 (5′-GC GTC TTT GTG ATC ATG CCT TCC GGC GTC G-3′) and JS20 (antiparallel) (5′-GCC GGA AGG CAT GAT CAC AAA GAC GCC G-3′). The PCR conditions used were as follows: 1 cycle of 1 min at 96 °C; 10 cycles of 30 s at 96 °C, 1 min at 60 °C, and 8 min at 68 °C; followed by 10 cycles of 30 s at 96 °C, 1 min at 55 °C, and 8 min at 68 °C. The plasmids encoding the mutations T116Y, T116E, E142Q, H218N, D120N, N28A, and K42M have been named pJSTB2, pJSTB3, pJSTB4, pJSTB5, pJSTB6, pJSTB7, and pJSTB8, respectively. All eight mutant plasmids were sequenced at the Nucleic Acid and Protein Services (NAPS), University of British Columbia, to verify that the desired base changes had taken place and that no unintentional base changes were introduced during PCR. The plasmid encoding for the H97N mutant was prepared by Anne Johnson as reported earlier (*1*).

Overexpression and Purification of WT and Mutant Epimerases. The WT and mutant epimerases were overexpressed in *E. coli* Y1090, a strain lacking a functional epimerase gene, as previously described (*1*). The purification procedure was modified slightly as indicated below. Following cell lysis, the proteins were partially purified by ammonium sulfate precipitation at 40% saturation. The precipitate was collected by centrifugation at 8000 rpm for 20 min, resuspended in buffer A (10 mM potassium phosphate buffer, pH 7.0, containing 10% glycerol), and dialyzed twice against 600 mL of buffer A using 12−14 kDa MWCO dialysis tubing (Spectrum). The partially purified proteins were then loaded on a 100 mL anion exchange DE-52 cellulose (Whatman) column preequilibrated with buffer A at room temperature. The column was first washed with buffer A and then eluted with a linear gradient of NaCl in buffer A (1 L, 0−0.4 M). Fractions containing the epimerase were identified by SDS−PAGE, pooled, concentrated, and desalted by dialysis against buffer A. Portions (≈35 mg) were applied to a 5 mL Hi Trap Q Sepharose HP anion exchange column (Pharmacia) that had been preequilibrated with buffer B (10 mM potassium phosphate buffer, pH 7.6, containing 10% glycerol) at room temperature. The proteins were then eluted with a linear gradient of NaCl in buffer B (0−0.4 M), and fractions containing the desired protein were pooled and frozen rapidly with liquid nitrogen. The purity of the wild-type epimerase and the mutants was determined to be >95% by SDS−PAGE. The mass of the purified enzymes was determined by ESI-MS, and CD spectra were collected in both the near- and far-UV regions to confirm the mutants were properly folded. The concentration of the epimerase was determined using A_{280} (1.73 mL mg^{-1} cm^{-1}). All procedures were carried out at 4 °C, unless otherwise specified.

Preparation of Zinc-Substituted Enzymes. The WT and mutant apoenzymes were prepared by incubating the enzymes in buffer B with 20 equiv of EDTA for 6 h. The excess EDTA was removed by extensive dialysis against metal-free HEPES−Tris buffer (50 mM, pH 7.6, containing 10% glycerol) using 12−14 kDa MWCO dialysis tubing (800 mL for 12 h and then 800 mL for 6 h). The apoenzymes were then reconstituted with 4 equiv of 99.99% pure $ZnCl_2$ and dialyzed once against metal-free HEPES−Tris buffer (800 mL for 6 h). For the H97N mutant, the apoenzyme was reconstituted with 2 equiv of $ZnCl_2$ and was not dialyzed after that. The metal-free buffer was prepared as described previously (*1*).

Cloning and Purification of L*-Ribulokinase.* The gene for L-ribulokinase, *araB*, was directly amplified from *E. coli* DH5αF′ genomic DNA. The primers used for amplification of *araB* were PMRK03 (5′-GGG AAT TCC CAT GGC GAT TGC AAT TGG CCT CGA T-3′) and PMRK02 (antiparallel) (5′-GTA GGG ATC CTG CAG TTA TAG AGT CGC AAC GGC-3). The primers were designed to introduce a *Nco*I restriction site at the 5′-end of *araB* and *Bam*HI and *Pst*I restriction sites at the 3′-end of *araB*. These restriction sites were then used to ligate *araB* into the pTrc99A prokaryotic expression vector using T4 DNA ligase. The resulting plasmid, pABT01, was sequenced at the Nucleic Acid and Protein Services Unit (NAPS), UBC, to ensure that *araB* was inserted without any errors. The plasmid pABT01 was transformed into $CaCl_2$-competent *E. coli* JM109, and the cells were grown in LB media containing 100 μg/mL ampicillin. The cells were grown at 37 °C to an OD_{600} of 0.6−0.8, induced with 5 mM IPTG, and then allowed to grow to an OD_{600} of 1.5−2.0. The cells were harvested by centrifugation at 5000 rpm for 20 min and then resuspended in 50 mM Tris−acetate buffer, pH 7.9 (containing 10% glycerol, 2 mM DTT, 1 mM EDTA, 1 μg/mL pepstatin, 1 μg/mL aprotinin, and 1 mM PMSF). The cells were lysed using a precooled French pressure cell at 20 000 psi, and the cell debris was removed by centrifugation at 8000 rpm for 30 min. Analysis by SDS−PAGE before and after induction indicated that the expressed protein accounted for about 10% of the total soluble protein. A sample of the ribulokinase was partially purified on a DE-52 column (elution with a linear gradient of 0−0.2 M NaCl in 50 mM Tris−acetate, pH 7.9, 10% glycerol containing 2 mM DTT). The mass of the protein was determined by ESI-MS, and the protein was characterized by N-terminal sequence analysis at the Nucleic Acid and Protein Service Laboratory (NAPS), UBC. An assay for ADP production (*9*) showed a specific activity of 1.9 units/mg at 2 mM L-ribulose and 1 mM ATP (37 mM Tris-HCl, pH 8.6).

Synthesis of L*-Ru5P.* L-Ribulose was prepared according to the procedure of Anderson (*10*). L-Arabinose (25 g) was refluxed in dry pyridine (200 mL) for 4 h. The pyridine was evaporated down to 50 mL, and the unreacted L-arabinose was removed by precipitation with ethanol. The filtrate was evaporated to give crude L-ribulose (2.5 g) as a brown oil that was used in the enzymatic synthesis of L-Ru5P without further purification.

A crude ribulokinase sample was prepared by growing *E. coli* Y1090 (pABT01) in 200 mL of LB medium containing 100 μg/mL ampicillin. The cells were grown at 37 °C to an OD_{600} of 0.6−0.8, induced with 5 mM IPTG, and then

allowed to grow to an OD_{600} of 1.5−2.0. The cells were harvested by centrifugation at 5000 rpm for 20 min and then resuspended in 1 mM glutathione (reduced) buffer, pH 7.0, containing 1 mM EDTA. The cells were lysed using a precooled French pressure cell at 20 000 psi, and the cell debris was removed by centrifugation at 8000 rpm for 30 min.

Crude L-ribulose (0.6 g, ≈4 mmol) was phosphorylated using half of the ribulokinase preparation and ATP according to the procedure of Anderson (*10*), and the resulting L-Ru5P was purified as described previously (*1*). The L-Ru5P was found to be greater than 90% pure as judged by ^{1}H NMR spectroscopy. Concentrations of L-Ru5P solutions were determined enzymatically using the epimerization assay conditions in the presence of an excess of L-Ru5P 4-epimerase (0.15 unit/mL).

Synthesis of Glycolohydroxamate. Benzyloxyacetyl chloride (3 g, 16.2 mmol), benzyloxyamine (4 g, 32.4 mmol), and triethylamine (18.5 mL) were refluxed in 150 mL of CH_2Cl_2 at 0 °C for 4 h under an argon atmosphere. The solution was washed with 1 N HCl and saturated sodium bicarbonate and then evaporated to dryness under reduced pressure. Purification by silica gel chromatography (3:7 EtOAc/hexane) gave 2.2 g (50%) of dibenzylated glycolohydroxamate as a white solid: ^{1}H NMR ($CDCl_3$) δ 8.75−8.85 (br s, 1 H, NH), 7.2−7.4 (m, 10 H), 4.9 (s, 2 H), 4.5 (s, 2 H), 4.1 (s, 2 H); LSIMS 272 ($M+H^+$). The dibenzylated glycolohydroxamate (2.2 g, 8.1 mmol) was dissolved in 10 mL of EtOAc, and 0.22 g of 10% Pd/C was added. The mixture was stirred under 1 atm of hydrogen at room temperature for 10 h and then filtered. The filtrate was evaporated to dryness under reduced pressure to give 700 mg (95%) of glycolohydroxamate as a light yellow oil: ^{1}H NMR (D_2O) δ 4.1 (s, 2 H); DCI-MS 92 ($M+H^+$).

Epimerization Assay Conditions. The epimerization reaction was assayed in the L-Ru5P to D-Xu5P direction at 37 °C by a method similar to that reported in the literature (*11*). The assay mixture contained 25 mM Gly-Gly buffer (pH 7.6), 0.125 mM $ZnCl_2$, 5 mM ribose 5-phosphate, 0.1 mM TPP, 0.15 mM NADH, 0.25 unit of transketolase, 2.5 units of α-glycerophosphate dehydrogenase (α-GDH), 25 units of triosephosphate isomerase, 0.005 unit of L-Ru5P 4-epimerase (Zn^{2+}-substituted), and varying amounts of L-Ru5P. Cuvettes were preincubated for 10 min prior to initiation to allow an impurity of an alternate substrate in the L-Ru5P (approximately 3%) to be consumed by the coupling enzymes. The reaction was initiated by the addition of the epimerase and followed by the decrease in absorbance of NADH at 340 nm ($\epsilon_{340} = 6.22\ mM^{-1}\ cm^{-1}$). The initial reaction velocities were fitted to the Michaelis−Menten equation using the program Graffit to obtain the kinetic constants.

Continuous Assay for Aldolase Activity. The Ca^{2+} salt of glycolaldehyde phosphate was prepared according to the method of Müller et al. (*12*) and converted to the sodium form as described previously (*1*). The continuous aldolase assay was similar to the epimerase assay; however, 5 mM glycolaldehyde phosphate and 50 mM dihydroxyacetone (DHA) were added as the substrate, and a large amount of L-Ru5P 4-epimerase (0.3−0.5 mg) had to be added to see a measurable rate. The Zn^{2+}-substituted enzyme was used, and 0.125 mM $ZnCl_2$ was included in all cases except for K42M in which the enzyme was used as initially purified and no $ZnCl_2$ was added. The reaction was initiated by adding DHA since glycolaldehyde phosphate appeared to be an alternate substrate for α-GDH. Each cuvette containing the assay mixture was first allowed to equilibrate at 37 °C for 5 min. The background rate due to glycolaldehyde phosphate was measured in the first 5 min of the reaction, and then the aldolase reaction was initiated by adding DHA. The background rate was subtracted from the final steady-state rate to obtain the rate of aldolase reaction.

X-ray Crystallography. The crystallization and data collection procedures for the D120N mutant were identical to those reported with the wild-type enzyme (*7*). The data were collected at the X12C beam line of NSLS and were 93.9% complete to 2.1 Å resolution. The mutant structure was refined with CNS to an *R*-factor/free *R*-factor of 0.205/0.251 using the wild-type structure as a starting model.

Substrate Docking Study. L-Ru5P and D-Xu5P were docked into the static epimerase structure using Dock Vision Version 1.0.3 (*13*), allowing conformational freedom for the substrates only. Manual optimization was performed using X-fit (*14*).

RESULTS

Residues Targeted for Mutagenesis. Three groups of residues in the active site of the epimerase were targeted for site-directed mutagenesis studies. The first were those that aligned with the putative acid/base catalysts of the aldolase in a sequence comparison. In addition to potentially identifying important catalytic residues in the epimerase, it was thought that by reintroducing the aldolase side chains back into the epimerase one might dramatically increase the background aldolase activity. At the time the work was initiated, reports on the aldolase−phosphoglycolohydroxamate complex structure implicated Glu73 and Tyr113′ as the residues important for acid/base catalysis (*4*, *5*). The corresponding residues in the epimerase are Asp76 and Thr116′, and the following mutants were constructed: D76N [from (*1*)], D76E, T116E, and T116Y.

The second group was chosen in an attempt to identify the phosphate-binding pocket of the epimerase. As discussed in the preceding paper, five conserved residues were implicated as serving this role due to both their sequence homology and their structural similarity with the corresponding residues in the aldolase (*7*). One of these, Asn28, was targeted for mutagenesis. In addition, the epimerase places Lys42 at the bottom of this putative pocket, and this residue may help bind the substrate via electrostatic interactions. The aldolase has no cationic counterpart in a comparable position. The mutants N28A and K42M were constructed to test these notions.

The final group of mutants focused on residues that could play the role as acid/base catalysts and serve to deprotonate the hydroxyls of the epimeric substrates in the two reaction directions (Figure 1). An inspection of the active site structure revealed that Asp76, Asp120′, Glu142, and His218′ were the only reasonable candidates to fulfill these roles and the mutants D76N [from (*1*)], D120N, E142Q, and H218N were therefore prepared. It should be noted that the eight C-terminal residues (224−231) were disordered and could not be located in the X-ray structure of the enzyme, yet they are likely forming a cap on the active site of an adjacent subunit

Table 1: Kinetic Constants for L-Ru5P with WT and Mutant L-Ru5P 4-Epimerases

	k_{cat} (s^{-1})	K_m (mM)	k_{cat}/K_m (s^{-1} mM^{-1})
wild type[a]	19.4 ± 0.4	0.047 ± 0.006	415
D76N[b]	0.16	0.14	1.2
D76E[a]	1.0 ± 0.03	0.25 ± 0.02	4.0
N28A[a]	2.5 ± 0.2	1.2 ± 0.2	2.1
K42M[a]	−	>2.0	0.032
D120N[a]	0.0057 ± 0.002	0.28 ± 0.02	0.020
H218N[a]	0.81 ± 0.02	0.58 ± 0.04	1.4
E142Q[a]	2.14 ± 0.02	0.086 ± 0.002	25
Y229F[c]	0.0118 ± 0.0003	0.129 ± 0.012	0.0915

[a] Reaction mixtures contained 25 mM Gly-Gly (pH 7.6), 0.125 mM $ZnCl_2$, and Zn^{2+}-substituted enzymes. [b] Data taken from (*1*). [c] Data taken from (*3*).

(*7*). Of these eight residues, only Tyr228 and Tyr229 could be capable of acting as acid/base catalysts and are conserved among the epimerases. Previous work by Cleland and coworkers showed that the mutation of Tyr229 to Phe resulted in a dramatically crippled enzyme, whereas the mutation of Tyr228 to Phe led to only moderate decreases in activity (*3*).

The mutations were introduced using PCR-based mutagenesis, and the resulting plasmids were fully sequenced to ensure they were free of any additional errors. In each case, the mutants were analyzed by ESI-MS to ensure that their molecular weight was as expected. Prior to kinetic analysis, the purified enzymes were converted into the apoenzyme form by dialysis against EDTA and then reconstituted with Zn^{2+} to ensure a homogeneous metal ion content.

Kinetic Analyses of Epimerase and Aldolase Activities. The mutant enzymes were assayed for epimerase activity in the L-Ru5P to D-Xu5P direction in the presence of 0.125 mM Zn^{2+}, and the results are outlined in Table 1 [data for D76N and Y229F were taken from references (*1*) and (*3*), respectively]. The largest decreases in the value of k_{cat} are observed with D120N and Y229F (0.0057 and 0.0118 s^{-1}, respectively, as compared to 19.4 s^{-1} for the wild-type enzyme). The largest increases in the value of K_M were observed with N28A and K42M. The former showed a value of 1.2 mM (as compared to 0.047 mM for the wild-type enzyme), and the latter could not be saturated under reasonable substrate concentrations (the Michaelis−Menten plot was completely linear up to 2.5 mM L-Ru5P). Kinetic constants were not determined for T116E and T116Y as these mutants were completely inactive.

Selected mutants were also examined for residual aldolase activity. In past work, the aldolase activity has been measured using a stopped assay that followed the rate of production of the epimeric pentose phosphates (L-Ru5P and D-Xu5P) from 50 mM dihydroxyacetone and 5 mM glycolaldehyde phosphate (*1*, *3*). This assay suffered from the fact that the pentose phosphate products bound much more tightly than the substrates and were therefore potent competitive inhibitors. To avoid this problem, the aldolase activity was measured using a continuous spectrophotometric assay for D-Xu5P that was a modification of the normal epimerase assay in which the substrate L-Ru5P was replaced with dihydroxyacteone and glycolaldehyde phosphate. One key to making this assay work was the realization that glycolaldehyde phosphate was a slow, alternate substrate for one of the coupling enzymes, α-glycerophosphate dehydrogenase (α-GDH), and therefore led to a background rate of NADH oxidation. By reducing the amount of added α-GDH from 5 units/mL (*11*) to 2.5 units/mL, and by keeping the concentration of glycolaldehyde phosphate at or below 5 mM, it was possible to keep this reaction at acceptable levels and still maintain coupled conditions. One drawback to this assay is that it only detects the production of D-Xu5P whereas the epimerase is presumably forming both epimers in its background aldol reaction. In the case of the wild-type enzyme and most of the mutants, the epimerase activity is still much greater than the background aldolase activity, and therefore any L-Ru5P that is formed will readily be epimerized and detected by this assay. In assays of mutants that have extremely low levels of epimerase activity, however, the observed rate may reflect the rate of formation of only D-Xu5P as opposed to that of total pentose phosphate. Despite these limitations, the assay does not suffer from competitive inhibition since the products are continuously removed by the action of the coupling enzymes. The observed aldolase activities using 50 mM dihydroxyacetone and 5 mM glycolaldehyde phosphate are shown in Table 2 and data for the additional mutant H97N have been included in order to clarify earlier conflicting reports (see Discussion). A surprising observation was that most of the mutants displayed a background aldolase activity similar to that of the wild-type enzyme (0.0085 μmol min^{-1} mg^{-1}). The largest difference was a 15-fold decrease in activity for H218N. The threonine mutants T116E and T116Y were found to be completely inactive using this assay (not shown in Table 2).

Table 2: Aldolase Activity with Glycolaldehyde Phosphate and Dihydroxyacetone[a]

enzyme	aldolase sp act. (μmol min^{-1} mg^{-1})	enzyme	aldolase sp act. (μmol min^{-1} mg^{-1})
wild type	8.5×10^{-3}	D120N	1.2×10^{-3}
D76E	1.1×10^{-3}	H218N	0.55×10^{-3}
N28A	6.1×10^{-3}	E142Q	12.2×10^{-3}
K42M[b]	1.4×10^{-3}	H97N	6.3×10^{-3}

[a] Reaction mixtures contained 0.125 mM $ZnCl_2$, 50 mM dihydroxyacetone, and 5 mM glycolaldehyde phosphate in 25 mM Gly-Gly (pH 7.6). [b] Excess Zn^{2+} was found to inhibit the aldolase activity for this mutant, so the enzyme was used directly as purified, and Zn^{2+} was omitted from the assay.

Attempts to fully delineate the kinetics of the background aldolase activity of the wild-type enzyme using the coupled assay were unsuccessful due to an extremely high value of K_M for dihydroxyacetone (>100 mM). It was evident, however, that at saturating levels of glyceraldehyde phosphate (5 mM) the value of αK_M for dihydroxyacetone decreased to about 50 mM.

Crystallographic Analysis of the D120N Mutant. The kinetic analyses presented above indicate that Asp120′ is a key active site residue since the D120N mutant showed dramatic reductions in the value of k_{cat} for epimerization. To probe whether this effect is structural in origin, the D120N mutant was crystallized, and its structure was solved using X-ray diffraction methods. The mutant was found to be structurally indistinguishable from the wild-type enzyme and showed a root-mean-squared deviation of only 0.28 Å over all the atoms of the ordered residues 1−223 in a monomer-wise comparison (Figure 2). A similar tetramer-wise com-

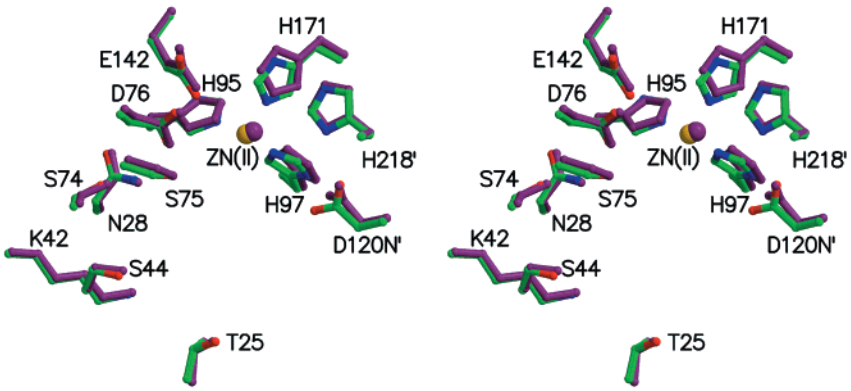

FIGURE 2: Stereoview showing the superposition of the wild-type and D120N active sites. The zinc ion and the neighboring side chains are shown. For the wild-type L-Ru5P 4-epimerase, the zinc, carbon, oxygen, and nitrogen atoms are colored in gold, green, red, and blue, respectively. For the D120N mutant, all atoms are colored in beet.

parison showed a root-mean-squared deviation of only 0.3 Å. Furthermore, none of the active site residues showed any significant perturbations.

Inhibition Study. Phosphoglycolohydroxamate is known to be a potent inhibitor of L-Fuc1P aldolase ($K_i = 3.1$ μM) as it mimics the enolate of dihydroxyacetone phosphate (*4*, *5*). Cocrystallization of this inhibitor with the aldolase led to a detailed picture of how the reaction intermediate likely binds to the aldolase. In the case of L-Ru5P epimerase, the corresponding inhibitor would be glycolohydroxamate since it should mimic the enolate of dihydroxyacetone. Glycolohydroxamate was prepared in 40% overall yield by the condensation of benzyloxyacetyl chloride and benzyloxyamine followed by deprotection with catalytic hydrogenation. To use the coupled assay for inhibition studies, it was first necessary to determine whether the hydroxamate interfered with the action of the coupling enzymes [particularly triosephosphate isomerase which is known to be inhibited by phosphoglycolohydroxamate (*15*)]. When D-Xu5P was used as a substrate in the coupled assay and 5 mM glycolohydroxamate was added, a notable inhibition of NADH consumption was observed. However, when the amount of added inhibitor was kept below 0.1 mM, no inhibition could be detected. Studies on the inhibition of L-Ru5P epimerase were then performed keeping the hydroxamate concentration below 0.1 mM, and no significant inhibition could be detected. To check whether synergistic binding was important, the study was repeated with 0.1 mM glycolohydroxamate and 1 mM glycolaldehyde phosphate; however, no synergistic inhibition could be detected.

Substrate Docking Study. Molecular mechanics studies were then performed in which L-Ru5P and D-Xu5P were docked into the active site of the epimerase in order to formulate a model for substrate binding. As discussed in the preceding paper, the observed structure of the epimerase most closely resembles that of the aldolase−phophoglycolohydroxamate complex, and therefore its conformation may closely resemble that of the Michaelis complex (*7*). The docking procedure allowed for translocation and single bond rotation of the substrates only. Candidate structures were picked from the priority list of lowest energy conformations in which the phosphate was located in the phosphate-binding pocket and both the carbonyl and C-3 hydroxyl were located within 4 Å of the zinc. Manual modeling was then used to optimize the zinc−oxygen bond distances so that they agreed with those observed in the aldolase−phophoglycolohydroxamate complex (1.9 and 2.2 Å, respectively). In addition, the C1−C2 bond was rotated such that the C-1 hydroxyl occupied the position of a water molecule that forms a hydrogen bond with Glu142 in the native structure. The resulting model of the complexes supports the notion that Tyr229′ and Asp120′ could function as the catalytic acid/base residues (Figure 3).

DISCUSSION

The evolutionary link between L-ribulose-5-phosphate 4-epimerase and L-fuculose-1-phosphate aldolase is clearly evident from sequence comparisons, mechanistic studies, and structural studies. Both enzymes belong to a superfamily that shares the ability to promote carbon−carbon bond cleavage reactions and stabilize enolate intermediates using a divalent cation. Despite these similarities, the enzymes must preserve subtle, yet important, differences in order to accommodate their respective substrates and catalyze their respective reactions. Both enzymes must position the C-2 carbonyl of the substrate in close proximity to the zinc, and position at least one acid/base catalytic residue appropriately for deprotonation of a C-4 hydroxyl. This must be done, however, on substrates in which the phosphates occupy dramatically different positions (C-5 in L-Ru5P and C-1 in L-Fuc1P). If both enzymes were to employ the same phosphate-binding pocket, they would have to bind the substrates in reversed or "flipped" orientations, and it would be unlikely that they could share common catalytic residues. The mutagenesis studies outlined in this paper help to share some light on the similarities and differences between the two catalytic strategies.

Initial reports on the L-Fuc1P aldolase structures indicated that Glu73 and Tyr113′ could serve as the catalytic acid/base residues in that enzyme (*4*, *5*). Sequence alignments [Figure 6 in ref (*7*)] showed that the corresponding residues in the epimerase were Asp76 and Thr116′, respectively, and that these are both conserved among the known epimerases. Later mutagenesis studies on L-Fuc1P aldolase ruled out the involvement of Tyr113′ since the appropriate mutants showed only modest decreases in catalytic activity (*6*). Instead, it appears that the aldolase only requires one active site residue, Glu73, to serve as both the required acidic and basic catalyst. To test whether Asp76 plays a similar role in the epimerase, D76N was examined. The value of k_{cat} for this mutant was

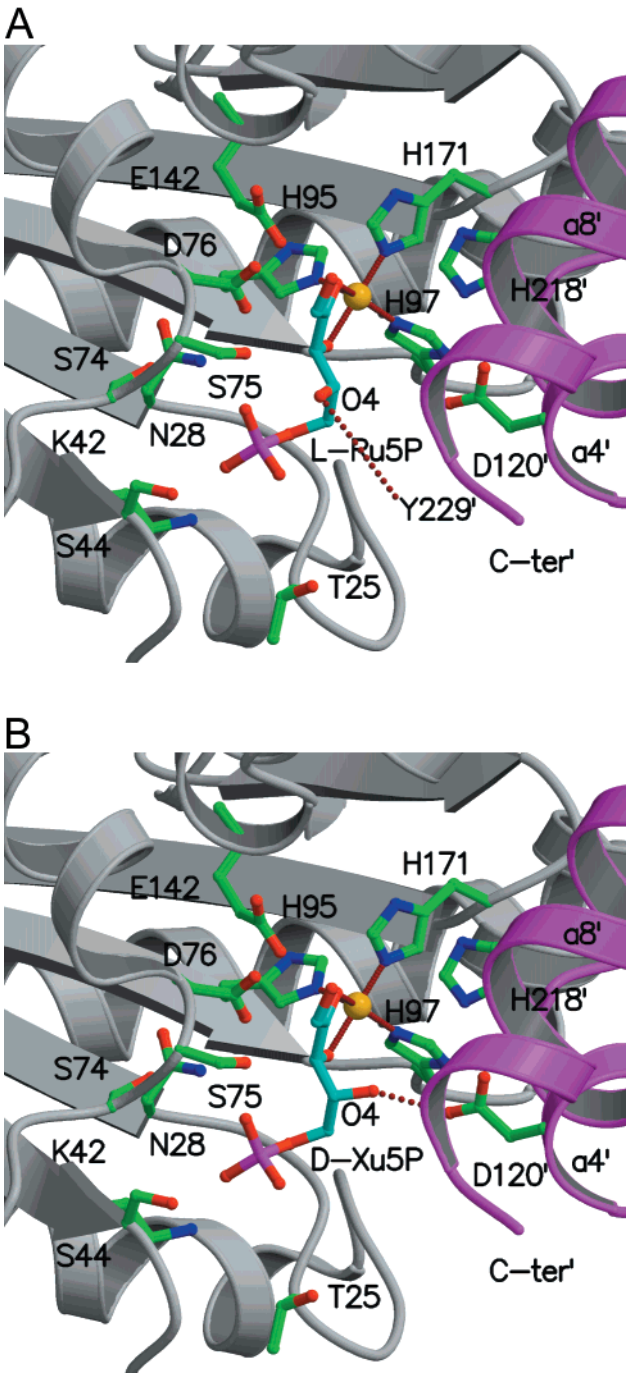

FIGURE 3: Ribbon views of the substrate-binding sites of L-Ru5P 4-epimerase with bound substrates (A) L-Ru5P and (B) D-Xu5P based on molecular models of the complexes. The secondary structural elements from two adjacent monomers that form the active site are shown in gray and magenta, respectively. Active site residues are shown in a ball-and-stick representation with green carbon, red oxygen, and blue nitrogen atoms. Residues that protrude from the second monomer are labeled with a prime symbol. The substrates are colored with cyan carbon, red oxygen, and magenta phosphate atoms. The substrates both provide two hydroxyls for coordination to the zinc ion.

found to decrease by a factor of only 200, and the value of K_M was relatively unaffected (Table 1). The decrease in activity indicates the residue is important for catalysis, but the magnitude of the change does not support the notion that it is required as a key acid/base residue. It is likely that the residue plays an electrostatic role during catalysis and is part of the metal's second-shell coordination sphere in the free enzyme. The latter notion is consistent with previous studies that indicated this mutant displays a reduced affinity for zinc. Thus, the epimerase has recruited different active site residues to serve as catalytic acids and bases.

Asp76 and Thr116′ mutants were also investigated as candidates that might display an increased residual aldolase activity. Since Asp76 aligns with the catalytic Glu73 of the aldolase, the mutant D76E was prepared. Increasing the length of the side chain by one methylene group may permit this residue to protonate the metal-bound enolate and generate the aldol products. The resulting kinetic values for both epimerase (Table 1) and aldolase activities (Table 2), however, were similar to those obtained for the wild-type enzyme. It is likely that the glutamate side chain of this mutant remained deprotonated throughout the epimerase reaction. Similar logic led to the investigation of T116E and T116Y; however, both mutants lacked any detectable epimerase or aldolase activity. It is likely that the increased steric bulk introduced by the mutations caused a conformational change that was incompatible with catalysis. This notion was supported by observed differences between the CD spectra of these mutants and the wild-type enzyme (data not shown) and by inspection of the X-ray structure that shows Thr116′ is 100% buried at the tetrameric interface by contacts with Tyr141, His97, and His171 of the neighboring monomer. In light of the recent report indicating that Tyr113′ is not a catalytic residue in the aldolase, no further studies were performed with Thr116′ epimerase mutants.

The results obtained with N28A and K42M support the notion that both enzymes utilize the same phosphate-binding pocket. Asn28 is a strictly conserved residue in both enzymes, and its counterpart (Asn29) forms a hydrogen bond with the phosphate of phosphoglycolohydroxamate in the aldolase−inhibitor complex (*5*). The N28A mutant had a very high K_M value (1.2 mM) and a k_{cat} value that was only 8-fold lower than wild-type enzyme, as expected for a mutant with decreased affinity for the substrate. Lys42 is located just below the phosphate-binding pocket of the epimerase; however, no counterpart is found at the comparable position in the aldolase. The extremely high value of K_M with K42M indicates that substrate binding has been impaired and is consistent with the idea that the positive charge is important for recognizing a negatively charged phosphate. It should be noted that the K_M value of the wild-type epimerase (0.047 mM) is significantly lower than that of the aldolase (2.2 mM), presumably because of this additional interaction.

When one compares the substrates L-Ru5P and L-Fuc1P, the distance from the C-2 carbonyl to the phosphate could be expected to be greater in the former, and therefore the distance from the metal ion to the phosphate-binding pocket should be greater in the epimerase. Indeed, the distance from the zinc to the phosphate in the docked L-Ru5P epimerase model (Figure 2) is 7.0 Å whereas the same distance in the aldolase−phosphoglycolohydroxamate structure is 6.5 Å.

The remaining candidates that could serve as acid/base catalysts in the epimerase reaction include Asp120′, His218′, Glu142, and the two tyrosines (Tyr228′ and Tyr229′) in the disordered C-terminal tail. D120N displayed a k_{cat} value that was reduced 3000-fold from that of the wild type and is likely functioning as an acid/base residue. On the other hand, the mutants H218N and E142Q displayed k_{cat} values that were

reduced from that of the wild type by only 24-fold and 9-fold, respectively, and therefore do not appear to fill this role (Table 1). The structure of the epimerase indicates that His218′ is hydrogen-bonded to Asp120′ and therefore the 24-fold reduction in the value of k_{cat} could reflect a loss in its ability to assist this residue in catalysis. In addition, H218′ forms a strong hydrogen bond to the side chain hydroxyl of the conserved Tyr141 in the adjacent monomer, which may serve to stabilize the active site. Similarly, E142 makes a salt bridge with R221′ and may serve to stabilize the active site interface. Both tyrosines were mutated previously by Cleland and co-workers, who saw a 1700-fold decrease in the value of k_{cat} for Tyr229′ and concluded that this residue was the other acid/base residue (*3*). It is interesting to note that both residues implicated as acid/base catalysts are supplied from an adjacent subunit of the epimerase and are replaced by aliphatic residues in the aldolase.

The dramatic reduction in activity observed with the D120N mutant could result from perturbing either a catalytically important residue or a structurally important residue. The observation that the structure of the D120N mutant is indistinguishable from that of the wild-type enzyme strongly supports the former case (Figure 2). It is difficult to see how the aspartate could serve as an electrostatic catalyst since the enolate intermediate is negatively charged. Instead, it seems more likely that Asp120′ acts as a catalytic acid/base residue.

The low levels of residual aldolase activity displayed by the epimerase served as one of the first pieces of evidence supporting the proposed retroaldol/aldol mechanism for this enzyme (*1*). It is quite puzzling, therefore, to see that this activity is relatively constant among the mutants prepared in this study. Mutants of the phosphate-binding pocket (K42M and N28A) as well as that of the catalytic residue (D120N) all showed aldolase activity that was within 10-fold of that observed with the wild-type enzyme (Table 2). Cleland and co-workers also observed the residual aldolase activity with this enzyme, and they found that Y229F showed a similar activity as the wild-type enzyme (*3*). One possible explanation could be that binding/release of the intermediates is the rate-determining step in this very slow reaction for both the mutants and the wild-type enzyme. The residual epimerase activity observed with the mutants shows that they are still capable of promoting carbon−carbon bond cleavage at a rate higher than the observed aldolase activity. Since the enzyme has evolved to avoid intermediate release, this barrier may be much higher than the barriers to catalysis even with the catalytically impaired mutants. A similar argument can be made if deprotonation/protonation of the dihydroxyacetone/enolate was the rate-determining step since this event is not a part of the normal catalytic process. At this point, it is unclear whether the deprotonation of dihydroxyacetone occurs in solution or in the enzyme active site. An alternate explanation is that the epimerase utilizes different catalytic residues and a different phosphate-binding pocket to promote the aldol addition of dihydroxyacetone to glycolaldehyde phosphate. This would be the case if the reaction does not occur in the active site; however, this seems unlikely given that the addition is slowed by severe product inhibition (vide infra). This could also happen if the aldolase activity arose from the binding of the pentose sugars/glycolaldehyde phosphate in an orientation that differs from the one it assumes during the epimerization reaction. An inspection of the active site reveals a potential alternate phosphate-binding pocket supplied by residues Arg221, Lys217, and Lys222. In this scenario, the altered orientation of binding could allow an acid/base residue to protonate the enolate and release the aldol products. During epimerization, however, the intermediates would be formed in the correct orientation and an acid/base residue would not be able to protonate the enolate.

Another aspect of the residual aldolase reaction that should be addressed is the activity of the mutant in which the metal ligand His97 was converted to Asn. Our initial report stated that H97N showed higher levels of aldolase activity than the wild-type enzyme, and we ascribed this to a mutation that caused the enzyme to become "sloppy" and permit protonation of the enolate intermediate (*1*). In subsequent work, Cleland and co-workers also reported that H97N showed aldolase activity but the rate was similar to that of the wild-type enzyme (*3*). We have used the coupled assay to quantify this activity and have shown that they do indeed have similar initial rates (Table 2). Our initial report was mistaken since the aldol reaction run in the direction of pentose phosphate formation is extremely sensitive to product inhibition and this is more severe in the case of the wild-type enzyme.

The mutagenesis studies described above support the notion that Asp120′ and Tyr229′ serve as the catalytic acid/base residues in the epimerization reaction, but give no clue as to which is responsible for deprotonating the hydroxyl of L-Ru5P and which is responsible for deprotonating the hydroxyl of D-Xu5P. In an attempt to address this matter, the substrate L-Ru5P was docked into the active site, and a low-energy conformation was analyzed. The chosen conformation placed the phosphate in the phosphate-binding pocket and positioned the C-2 carbonyl and C-3 hydroxyl appropriately for ligation to the zinc (Figure 3A). In the resulting model, the C-4 hydroxyl is pointing directly out of the active site cleft. If the disordered C-terminal tail formed a cap over this cleft, Tyr229′ could be positioned appropriately to deprotonate this hydroxyl. In the corresponding model of bound D-Xu5P, the stereochemistry at C-4 is reversed, and the C-4 hydroxyl is located within 3 Å of Asp120′ (Figure 3B). Thus, the modeling would predict that Tyr229′ is responsible for the deprotonation of L-Ru5P and Asp120′ is responsible for the deprotonation of D-Xu5P.

From the available structural and mechanistic studies, it is clear that the epimerase and the aldolase have evolved from a common ancestor and both have retained the ability to use a divalent cation in promoting carbon−carbon bond cleavage/formation reactions via a retroaldol/aldol process. They have also retained the use of a conserved phosphate-binding pocket that is required for substrate recognition. The different positioning of the phosphate in their respective substrates, however, dictates that the substrates must bind in a reversed or "flipped" orientation. For this reason, the enzymes have recruited completely different residues to serve as acids and bases during catalysis.

ACKNOWLEDGMENT

We thank Prof. W. W. Cleland for his insightful comments and for providing us with samples of transketolase.

REFERENCES

1. Johnson, A. E., and Tanner, M. E. (1998) *Biochemistry 37*, 5746−5754.
2. Lee, L. V., Vu, M. V., and Cleland, W. W. (2000) *Biochemistry 39*, 4808−4820.
3. Lee, L. V., Poyner, R. R., Vu, M. V., and Cleland, W. W. (2000) *Biochemistry 39*, 4821−4830.
4. Fessner, W.-D., Schneider, A., Held, H., Sinerius, G., Walter, C., Hixon, M., and Schloss, J. V. (1996) *Angew. Chem., Int. Ed. Engl. 35*, 2219−2221.
5. Dreyer, M. K., and Schulz, G. E. (1996) *J. Mol. Biol. 259*, 458−466.
6. Joerger, A. C., Gosse, C., Fessner, W.-D., and Schulz, G. E. (2000) *Biochemistry 39*, 6033−6041.
7. Luo, Y., Samuel, J., Tanner, M. E., and Strynadka, N. C. J. (2001) *Biochemistry 40*, 14763−14771.
8. Jones, D. H., and Winistorfer, S. C. (1992) *BioTechniques 12*, 528−535.
9. Anderson, M. S., Eveland, S. S., Onishi, H. R., and Pompliano, D. L. (1996) *Biochemistry 35*, 16264−16269.
10. Anderson, R. L. (1966) *Methods Enzymol. 9*, 48−51.
11. Davis, L., Lee, N., and Glaser, L. (1972) *J. Biol. Chem. 247*, 5862−5866.
12. Müller, D., Pitsch, S., Kittaka, A., Wagner, E., Wintner, C. E., and Eschenmoser, A. (1990) *Helv. Chim. Acta 73*, 1410−1468.
13. Hart, T. N., Ness, S. R., and Read, R. J. (1997) *Proteins: Struct., Funct., Genet., Suppl. 1*, 205−209.
14. McRee, D. E. (1999) *J. Struct. Biol. 125*, 156−165.
15. Collins, K. D. (1974) *J. Biol. Chem. 249*, 136−142.

BI011252V